**ChemComm RSC**Publishing

## COMMUNICATION

View Article Online

Cite this: Chem. Commun., 2013, 49 11436

Received 30th August 2013, Accepted 15th October 2013

DOI: 10.1039/c3cc46658h

www.rsc.org/chemcomm

## Iron oxide-loaded hollow mesoporous silica nanocapsules for controlled drug release and hyperthermia†

Feng Lu,‡ab Adriana Popa,‡a Shiwei Zhou,b Jun-Jie Zhu\*b and Anna Cristina S. Samia\*a

Magnetic field-responsive iron oxide-loaded hollow mesoporous silica nanocapsules that exhibit high drug loading capacity were synthesized using polymer nanospheres as sacrificial templates. Due to their magnetic field induced heating and remotely triggered drug release capabilities, these hybrid nanomaterials provide an excellent platform for the combination of hyperthermia and chemotherapy.

The unique physicochemical properties of nanoparticles provide a versatile platform for many biomedical applications, such as imaging, diagnosis, and drug delivery systems. Among the nanoparticles of interest, mesoporous silica nanoparticles (MSNs) have been widely investigated as potential drug carriers because of their large surface area, ease of surface modification and good biocompatibility.2 In particular, hollow MSNs have recently attracted increasing interest,2,3 due to their payload capacity and sustained release capability. When designing a MSN-based drug delivery system there are two main aspects, which are paramount and highly desirable for clinical applications that need to be addressed: (1) targeted delivery capability and (2) controlled release behaviour, which can remarkably improve the therapeutic efficiency (increase drug accumulation in target tissue) and greatly minimize side effects (lower drug accumulation in healthy tissue).5 Currently, the most explored approach for achieving controlled drug release using MSN carriers is through surface functionalization that entails derivatization with pH sensitive or biomolecule responsive gates. However, pH and biomolecular triggered release methods are challenging in practical applications because of the complexity

of the in vivo environment. In addition, these responsive gate coatings prevent further modification (e.g. functionalization with targeting moieties), which is essential for achieving tumor targeted delivery. Thus, triggering the release from inside the MSNs by an external and noninvasive physical stimulus and maintaining a functionalizable nanoparticle surface are highly desirable. Most recently, light enhanced drug release using photo-responsive Au nanorods<sup>5a</sup> and graphene<sup>5b</sup> loaded MSNs has been achieved. However, the practical application of phototriggered drug delivery systems can be limited due to the low tissue penetration depth of light (several mm for near infrared light). In comparison, human tissues are transparent to the magnetic field, thus the use of a magnetic field can serve as an alternative approach to overcome the limitations mentioned above. Herein, we encapsulated iron oxide nanoparticles (IONPs) inside hollow mesoporous silica shells, which enable the resulting nanocapsule drug delivery system to be responsive to an alternating magnetic field (AMF). The localized heat generated by the IONPs under AMF excitation can significantly promote drug release and ultimately raise the temperature of the surrounding media to clinical hyperthermia levels (41–46 °C) for potential cancer therapy applications. In addition, sustained drug release behaviour due to the hollow interiors of the host mesoporous silica structure was also observed. Therefore, the synthesized nanocapsules proved to be promising materials for combined hyperthermia and chemotherapeutic drug delivery applications.

The methodology used to prepare the hollow mesoporous silica nanocapsules that are loaded with IONPs is illustrated in Scheme 1. Briefly, oleic acid coated IONPs with an average diameter of 12 nm were embedded in a polymer layer via an emulsion polymerization method, according to a previously reported method with slight modifications. 10 The successful encapsulation of IONPs within the polymer nanospheres (94  $\pm$  8 nm) is evident from the TEM image shown in Fig. 1a. The polymer nanospheres were then used as templates for growing the silica coating using a sol-gel approach. 11 The obtained nanostructure exhibits a core-shell morphology with a silica shell thickness of  $\sim$  25 nm, as shown in Fig. 1b. The iron oxide-loaded

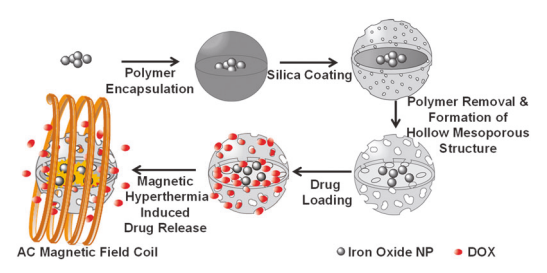
<sup>&</sup>lt;sup>a</sup> Department of Chemistry, Case Western Reserve University, 10900 Euclid Ave., Cleveland, OH, 44106, USA. E-mail: anna.samia@case.edu; Fax: +1 (216)368-3006; Tel: +1 (216)368-3852

<sup>&</sup>lt;sup>b</sup> State Key Lab of Analytical Chemistry for Life Science, School of Chemistry and Chemical Engineering, Nanjing University, Nanjing 210093, P. R. China. E-mail: jjzhu@nju.edu.cn; Fax: +86-25-8359-7204; Tel: +86-25-8359-7204

<sup>†</sup> Electronic supplementary information available: Experimental details, FT-IR spectra, powder X-ray diffraction data, magnetization and drug loading data. See DOI: 10.1039/c3cc46658b

<sup>‡</sup> These authors contributed equally to this work.

Communication ChemComm



Scheme 1 Schematic illustration of nanocapsule synthesis, drug loading and magnetic hyperthermia induced release

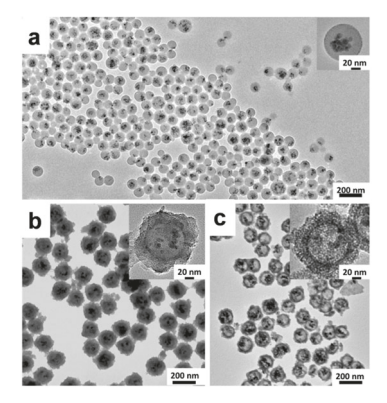


Fig. 1 (a) TEM images of polymer-encapsulated IONPs, (b) silica-coated polymerencapsulated IONPs, and (c) iron oxide-loaded hollow mesoporous silica nanocapsules. Insets: respective HR-TEM images of the nanoparticles during different fabrication stages.

hollow mesoporous silica nanocapsules were subsequently formed by heat treatment at 550 °C for 6 hours, which led to the simultaneous mesopore formation and removal of the organic polymer layer. FT-IR and powder X-ray diffraction analysis of the nanocapsules before and after heat treatment showed the effective removal of the polymer template and preservation of the IONPs phase after annealing (ESI,† Fig. S1). As revealed in the inset of Fig. 1c, randomly distributed mesopores were generated in the shell, and the distinct contrast between the shell and the nanomaterial interior confirmed the hollow structure. One exciting aspect of this preparative method is that it provides a modular synthesis approach with many tunable parameters, such as iron oxide nanoparticle loading, inner core size, silica shell thickness and pore size.3,10 Moreover, there is great potential for extending this fabrication method to make multi-functional hollow mesoporous silica nanomaterials with different types of encapsulated nanoparticles.

A typical IV isotherm (Fig. 2a) with a distinct hysteresis loop starting at  $P/P_0 = 0.4-0.5$  was observed from N<sub>2</sub> adsorptiondesorption measurements, demonstrating the mesoporous characteristics of the nanomaterial.2,12 The BET surface area and single-point total pore volume were measured to be 494 m<sup>2</sup> g<sup>-1</sup> and 0.533 cm<sup>3</sup> g<sup>-1</sup>, respectively, which are relatively large values for magnetic nanocomposites. 13 The pore size of the nanocapsules was calculated from the desorption branch of the isotherm and was found to be centered at 3.8 nm, as shown in the inset of Fig. 2a, and is consistent with what has been previously reported in the literature.<sup>2,3</sup> The magnetization

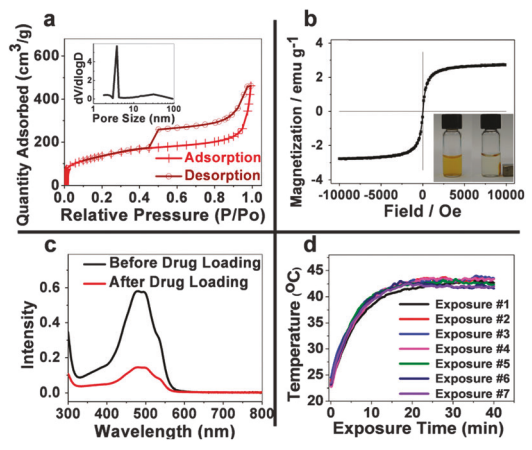


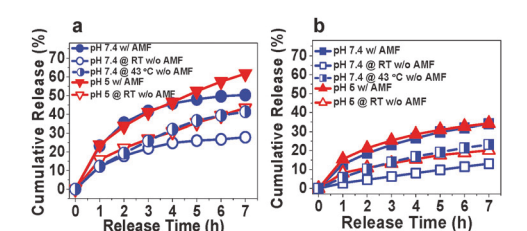
Fig. 2 (a) N<sub>2</sub> adsorption–desorption isotherms of the synthesized iron-loaded hollow mesoporous silica nanocapsules; inset: a pore size distribution plot. (b) Magnetization curve of the nanocapsules at 300 K; inset: photograph of the Dox-loaded nanocapsules and their response to an external magnet. (c) UV-Vis absorption spectra of Dox solution before and after loading in the nanocapsules. (d) Heating curves of the nanocapsule suspension under alternating magnetic field excitation during the 7 exposures of 40 min each.

properties of the nanocapsules were studied using a superconducting quantum interference device (SQUID) magnetometer (Fig. 2b). Neither coercivity nor remanence was observed in the magnetization curves of the nanocapsules, indicating that the superparamagnetic behaviour of the IONPs was maintained throughout the fabrication process (ESI, Fig. S2). Although the resulting overall magnetization of the IONPs decreased upon encapsulation inside the hollow mesoporous silica structure, the resulting hybrid nanocapsules still show a good response to an external magnet as shown in the inset of Fig. 2b.

To demonstrate the potential of the prepared nanocapsules for controlled drug delivery, doxorubicin hydrochloride (Dox), a common anticancer drug, was employed as a model drug to investigate the loading capacity, encapsulation efficiency and in vitro release rate. Large amounts of Dox can be loaded in the synthesized nanocapsules, which can be attributed to the large hollow interiors and strong electrostatic interaction between the positively charged Dox and the negatively charged silica surface.<sup>3,5b</sup> By increasing the concentration of Dox in solution, up to 385 mg of Dox was loaded per gram of the nanocapsules, which is higher than the amount that was loaded in solid mesoporous silica with a larger surface area.<sup>14</sup> However, the loading efficiency decreased as expected at high concentration of Dox from 97% for 97 mg  $g^{-1}$  loading to 70% for 385 mg  $g^{-1}$  loading.

When an alternating magnetic field was applied to the drug loaded system, the nanocapsule suspension showed a fast magnetic field response and the temperature of the suspension gradually raised up to 43 °C for a sample with a concentration of 1.3 mg mL<sup>-1</sup>. As the concentration of the nanocapsules was increased, the temperature of the media raised up to 46 °C (ESI,† Fig. S3). As mentioned above, this magnetic hyperthermia effect can be used as a therapeutic method for cancer treatment.

The Dox release from the synthesized nanocapsules with two different drug loading amounts (97 mg  $g^{-1}$ , Fig. 3a and 385 mg  $g^{-1}$ , Fig. 3b), was investigated in pH 7.4 and pH 5 Tris buffers.



ChemComm

**Fig. 3** Cumulative release of Dox with and without AMF at different pHs and temperatures for 97 mg  $g^{-1}$  (a) and 385 mg  $g^{-1}$  (b) drug loaded nanocapsules.

For the nanocapsules with the low Dox loading, the drug is expected to be mainly absorbed in the pores of the silica shell, thus showing a faster initial drug release at pH 7.4, followed by a plateau (Fig. 3a), which is similar to the release of Dox from solid MSNs.<sup>5b</sup> Lowering of the pH resulted in a slight increase in the release rate due to a decrease in the electrostatic interaction between payload and silica caused by the protonation of surface silanols at low pH values. 14 On the other hand, the nanocapsules with the high Dox loading showed continuous release behaviour at a nearly constant rate over 7 hours at both pH values (Fig. 3b), which could be attributed to the storage of a significant amount of drug inside the hollow cores. For both drug loadings, excitation with an AMF was found to greatly promote the release of Dox. The cumulative drug release under AMF exposure was about 1.8 and 2.6 times greater than that without the magnetic stimulus for the sample with 97 and 385 mg g<sup>-1</sup> Dox loading, respectively, within the 7 hour observation window. However, the influence of pH in the presence of the AMF was found to be negligible, but might be advantageous for magnetic field triggered drug release in complex bio-environments. Moreover, in order to demonstrate that the enhanced drug release was due to the local internal heating caused by the IONPs under AMF excitation, a control drug release experiment at 43 °C in the absence of AMF was performed. As shown in Fig. 3, the drug release at 43 °C is slightly higher than what was observed at room temperature, which can be explained by the accelerated diffusion of the Dox molecules throughout the pores of the nanocapsules at elevated temperature. However, an even more enhanced release rate can be seen under AMF excitation (Fig. 3). The observed accelerated drug release under AMF excitation can be attributed to the temperature gradient that develops between the internal cavity versus the outside environment of the nanocapsules, which in turn stimulates drug diffusion.15

In summary, we have described a modular approach to prepare multi-functional hollow mesoporous silica nanocapsules with encapsulated IONPs. The hollow mesoporous silica nanostructures provide a large drug loading capacity and sustained release property, while the loaded IONPs can serve as magnetic field responsive hyperthermia agents. Moreover, the magnetic field response of the synthesized nanocapsules can significantly promote the release of payload to the surrounding media. In addition, compared to other pH/biomolecular gate controlled systems, in our drug delivery system the silica surface remains available for further functionalization with targeting ligands. Thus, the synthesized hybrid nanocapsules provide a promising platform for the combination of hyperthermia and chemotherapy for cancer treatment applications.

AP is supported by a NASA Space Technology Research Fellowship (#NNX11AN69H). ACSS would like to acknowledge financial support from the Solid State and Materials Chemistry Division of NSF (CAREER Grant DMR-1253358). FL and JJZ would like to acknowledge support from the National Natural Science Foundation of China (No. 21020102038).

## Notes and references

- 1 (a) N. A. Frey, S. Peng, K. Cheng and S. Sun, Chem. Soc. Rev., 2009, 38, 2532; (b) M. H. Pablico-Lansigan, S. F. Situ and A. C. S. Samia, Nanoscale, 2013, 5, 4040.
- 2 (a) H. X. Wu, G. Liu, S. J. Zhang, J. L. Shi, L. X. Zhang, Y. Chen, F. Chen and H. R. Chen, J. Mater. Chem., 2011, 21, 3037; (b) N. Ž. Knežević, E. R. Hernández, W. E. Hennink and M. Vallet-Regi, RSC Adv., 2013, 3, 9584.
- 3 Y. Gao, Y. Chen, X. F. Ji, X. Y. He, Q. Yin, Z. W. Zhang, J. L. Shi and Y. P. Li, *ACS Nano*, 2011, 5, 9788.
- 4 J.-H. Lee, K.-J. Chen, S.-H. Noh, M. A. Garcia, H. Wang, W.-Y. Lin, H. Jeong, B. J. Kong, D. B. Stout, J. Cheon and H.-R. Tseng, *Angew. Chem.*, *Int. Ed.*, 2013, 52, 4384.
- 5 (a) Z. J. Zhang, L. M. Wang, J. Wang, X. M. Jiang, X. H. Li, Z. J. Hu, Y. H. Ji, X. C. Wu and C. Y. Chen, Adv. Mater., 2012, 24, 1418; (b) Y. Wang, K. Y. Wang, J. F. Zhao, X. G. Liu, J. Bu, X. Y. Yan and R. Q. Huang, J. Am. Chem. Soc., 2013, 135, 4799.
- 6 J. Lammertyn, A. Peirs, J. De Baerdemaeker and B. Nicolai, Postharvest Biol. Technol., 2000, 18, 121.
- 7 J. Tiihonen, R. Hari, M. Kajola, J. Karhu, S. Ahlfors and S. Tissari, Neurosci. Lett., 1991, 129, 303.
- 8 M. H. Cho, E. J. Lee, M. Son, J.-H. Lee, D. Yoo, J. Kim, S. W. Park, J.-S. Shin and J. Cheon, *Nat. Mater.*, 2012, **11**, 1038.
- 9 A. P. Khandhar, R. M. Ferguson, J. A. Simon and K. M. Krishnan, J. Appl. Phys., 2012, 111, 07B306.
- 10 X. L. Xu, G. Friedman, K. D. Humfeld, S. A. Majetich and S. A. Asher, Adv. Mater., 2001, 13, 1681.
- 11 Y. Lu, J. McLellan and Y. N. Xia, Langmuir, 2004, 20, 3464.
- 12 J. Kim, J. E. Lee, J. Lee, J. H. Yu, B. C. Kim, K. An, Y. Hwang, C. H. Shin, J. G. Park, J. Kim and T. Hyeon, J. Am. Chem. Soc., 2006, 128, 688.
- 13 J. P. Ge, Q. Zhang, T. R. Zhang and Y. D. Yin, Angew. Chem., Int. Ed., 2008, 47, 8924.
- 14 C. H. Lee, S. H. Cheng, I. P. Huang, J. S. Souris, C. S. Yang, C. Y. Mou and L. W. Lo, *Angew. Chem., Int. Ed.*, 2010, 49, 8214.
- 15 S. D. Kong, W. Zhang, J. H. Lee, K. Brammer, R. Lal, M. Karin and S. Jin, *Nano Lett.*, 2010, 10, 5088.